Video Article

Insect-controlled Robot: A Mobile Robot Platform to Evaluate the Odor-tracking Capability of an Insect

Noriyasu Ando[1], Shuhei Emoto[1], Ryohei Kanzaki[1]

[1]Research Center for Advanced Science and Technology, The University of Tokyo

Correspondence to: Noriyasu Ando at ando@brain.imi.i.u-tokyo.ac.jp

URL: http://www.jove.com/video/54802
DOI: doi:10.3791/54802

Keywords: Neuroscience, Issue 118, silkmoth, insect, odor-tracking, pheromone, vision, multisensory integration, insect-machine hybrid robot, biomimetics

Date Published: 12/19/2016

Citation: Ando, N., Emoto, S., Kanzaki, R. Insect-controlled Robot: A Mobile Robot Platform to Evaluate the Odor-tracking Capability of an Insect. *J. Vis. Exp.* (118), e54802, doi:10.3791/54802 (2016).

Abstract

Robotic odor source localization has been a challenging area and one to which biological knowledge has been expected to contribute, as finding odor sources is an essential task for organism survival. Insects are well-studied organisms with regard to odor tracking, and their behavioral strategies have been applied to mobile robots for evaluation. This "bottom-up" approach is a fundamental way to develop biomimetic robots; however, the biological analyses and the modeling of behavioral mechanisms are still ongoing. Therefore, it is still unknown how such a biological system actually works as the controller of a robotic platform. To answer this question, we have developed an insect-controlled robot in which a male adult silkmoth (*Bombyx mori*) drives a robot car in response to odor stimuli; this can be regarded as a prototype of a future insect-mimetic robot. In the cockpit of the robot, a tethered silkmoth walked on an air-supported ball and an optical sensor measured the ball rotations. These rotations were translated into the movement of the two-wheeled robot. The advantage of this "hybrid" approach is that experimenters can manipulate any parameter of the robot, which enables the evaluation of the odor-tracking capability of insects and provides useful suggestions for robotic odor-tracking. Furthermore, these manipulations are non-invasive ways to alter the sensory-motor relationship of a pilot insect and will be a useful technique for understanding adaptive behaviors.

Video Link

The video component of this article can be found at http://www.jove.com/video/54802/

Introduction

Autonomous robots capable of finding an odor source can be important for the safety and security of society. They can be used for the detection of disaster victims, of drugs or explosive materials at an airport, and of hazardous material spills or leaks in the environment. At present, we rely entirely on well-trained animals (*e.g.,* dogs) for these tasks, and robotic odor source localization has been strongly expected to relieve the workload of these animals. Finding an odor source is a challenging task for robots because odorants are distributed intermittently in an atmosphere[1]; therefore, continuous sampling of the odor concentration gradient is not always possible. Thus, a search strategy using intermittent odor cues is necessary for the achievement of robotic odor source localization[2-4].

Odor source localization is essential for organism survival and includes tasks such as finding food, mating partners, and sites for oviposition. To overcome the difficulty in tracking patchy distributed odorants, organisms have evolved various behavioral strategies consisting of two fundamental behaviors: moving upstream during odor reception and cross-stream during cessation of odor reception[5,6]. These reactive strategies have been well-documented in insects and further combined with other modalities, such as wind direction and vision[5-8]. The insect behavioral models have also been useful examples for robotics[3,9-11], in which behavioral algorithms or neural circuit models are implemented into mobile robots for the evaluation of odor source localization abilities[10,12-15]. From biomimetic perspectives, this "bottom-up" approach is certainly a fundamental way to develop biomimetic robots. However, the bottom-up approach is not a shortcut to obtaining a useful search strategy, because biological analyses are still ongoing, and the modeling of the sensory-motor systems behind insect behaviors has not been completed. Therefore, it is still unknown how such a biological system actually works as a controller of a robotic platform.

In this article, we demonstrate the protocol of a straightforward "top-down" approach to develop an odor-tracking mobile robot controlled by a biological system[16,17]. The robot is controlled by a real insect and can be regarded as a prototype of future insect-mimetic robots. In the robot's cockpit, a tethered adult male silkmoth (*Bombyx mori*) walked on an air-supported ball in response to the female sex pheromone, which was delivered to each antenna through air suction tubes. The ball rotations caused by the walking of the onboard moth were measured by an optical sensor and were translated into the movement of the two-wheeled robot. The advantage of this "hybrid" approach is that experimenters can investigate how the insect sensory-motor system works on the robotic platform where a pilot insect is in a closed loop between the robot and a real odor circumstance. The manipulation of the robotic hardware alters the closed loop; therefore, the insect-controlled robot is a useful platform for both engineers and biologists. For engineering, the robot represents the first steps of applying a biological model to meet the requirements for robotic tasks. For biology, the robot is an experimental platform for studying sensory-motor control under a closed loop.

Protocol

1. Experimental Animal

1. Prepare a plastic box to keep the pupae of male silkmoths (*B. mori*) until their eclosion. Put paper towels at the bottom and pieces of cardboard around the inner wall of the box (**Figure 1A**).
   Note: The pieces of cardboard are necessary for the adult moths to hold while extending their wings during eclosion (**Figure 1A**).
2. Put male silkmoth (*Bombyx mori*) pupae in the box and keep them in an incubator until eclosion under a 16-hr:8-hr light:dark cycle at 25 °C.
   NOTE: The male and female pupae can be discriminated by the sex markings on the abdomen (**Figure 1B**).
3. Collect adult male moths after eclosion and move them into a new box.
4. Keep the adult moths in an incubator under a 16-hr:8-hr light:dark cycle and decrease the temperature to 15 °C to reduce their activity before the experiment.

2. Tethering a Silkmoth

1. Fabrication of an attachment for tethering (**Figure 2A**)
   Note: The attachment consists of a copper wire with a strip of a thin plastic sheet at its tip. This ensures the dorsal-ventral movement of the thorax during walking (**Figure 2B**).
   1. Prepare a strip of a thin plastic sheet, 2 × 40 mm (thickness: 0.1 mm), and fold it in the middle.
   2. Attach the folded strip to the tip of a copper wire with an adhesive.
   3. Bend the tip of the folded strip where the thorax of a silkmoth is attached.

2. Use adult moths (2-8 days old) during the light period for the experiment.
   Note: The sensitivity to the pheromone strongly depends on the circadian clock[18]. Because *B. mori* is a diurnal moth, the experiment must be performed during the light period.
3. Gently remove all scales on the dorsal thorax (mesonotum) using a piece of wet tissue (or cotton swab) and expose the cuticle of the mesonotum (**Figure 2C**).
4. Paste an adhesive on the strip of plastic on the attachment and on the surface of the exposed mesonotum with a small flat-blade screwdriver and wait 5-10 min until the adhesive is no longer sticky.
   Note: The adhesive should not touch the wing hinge or the forewing tegulae (**Figure 2C**).
5. Bond the mesonotum to the attachment.
6. Keep the moth tethered before placing it inside the cockpit of the robot. Hold the attachment on a stand and put a piece of paper under the legs to rest the moth.

3. Insect-controlled Robot

1. Design the hardware of the insect-controlled robot based on previous works[16,17,19].
   Note: The insect-controlled robot consists of an air-supported treadmill with an optical mouse sensor to capture the insect locomotion, custom-built AVR-based microcontroller boards for processing and motor control, and two DC brushless motors (**Figures 3** and **4**). The robot can run on the basis of the ball rotation with 96% precision or higher, within a time delay of 200 msec. It also ensures the mobility of maximum forward speed (24.8 mm/sec) and angular velocity (96.3°/sec) of the silkmoth during pheromone tracking behavior[16]. The airflow of the treadmill (**Figure 5A**) and odor delivery system (**Figure 5B**) are designed for the onboard moth to walk smoothly on the ball and to acquire an odor by two antennae. The air intake and flow channel of the treadmill is separated from those of the odor delivery system to avoid contamination of the pheromone.
2. Design the software for the onboard microcontrollers based on previous works[16].
   Note: The onboard microcontroller calculates the robot movements from the insect locomotion measured with an optical sensor (rotational, Δx; translational, Δy; **Figure 6**). The travel distance (ΔL) and turn angle ($\Delta\theta$) per unit time of the robot are calculated on the basis of travel distance of each wheel (left, ΔL_L; right, ΔL_R) such as $\Delta L = (\Delta L_L + \Delta L_R) / 2$ and $\Delta\theta = (\Delta L_L - \Delta L_R) / D_{wheel}$, where D_{wheel} is the distance between the two wheels (120 mm). ΔL_L and ΔL_R are further described as $\Delta L_L = \Delta L_{x,L} + \Delta L_{y,L}$ and $\Delta L_R = \Delta L_{x,R} + \Delta L_{y,R}$, where $\Delta L_{x,L}$ and $\Delta L_{x,R}$ are the travel distances of the wheels on the left and right sides controlled by Δx, and $\Delta L_{y,L}$ and $\Delta L_{y,R}$ are those controlled by Δy. Ideally, $\Delta L_{x,L}$ and $\Delta L_{x,R}$ are described as $\Delta L_{x,L} = -\Delta L_{x,R} = G\,\Delta x\,(D_{wheel} / D_{ball})$, and $\Delta L_{y,L}$ and $\Delta L_{y,R}$ are described as $\Delta L_{y,L} = \Delta L_{y,R} = G\,\Delta y$, where G is the motor gain and D_{ball} is the diameter of the ball (50 mm). In practice, the motor gain is independently set by each side (left or right wheel) and by each direction (forward or backward rotation) so as to calibrate the robot movement. The independent gains further allow for the setting of asymmetrical motor rotation to generate a turning bias of the robot (see step 6.1).
3. Wash the surface of a white expanded polystyrene ball (mass: approximately 2 g; diameter: 50 mm) with water to remove any possible olfactory or visual cues.
   Note: The surface of a new ball should be roughed with fine-grit sandpaper, such as P400, which ensures the grip of the legs on the ball.
4. Turn on the blower fan that supplies air at 9 V to the treadmill and floats the ball (**Figure 5A**). Observe the ball float approximately 2 mm from the bottom of the cup.
5. Using a screw, attach the copper wire of the attachment with the moth (see step 2) to a fixture in the cockpit of the robot (see **Figure 3** inset). Make sure that the position of the middle legs is at the center of the ball (**Figure 7A**).
6. Adjust the vertical position of the attachment to enable the moth to walk normally on the ball. Keep the ball at the same height before and after attaching the moth (**Figure 7B**).
   Note: A too-low position of the attachment adds pressure on the moth and elicits backward walking to resist the pressure (**Figure 7C**), whereas a too-high position causes unstable walking and failures of the sensor due to changes in the vertical position of the ball (**Figure 7D**). To check normal walking behavior, a single-puffed pheromone stimulus is used to trigger walking in the moth (for the pheromone stimulus,

see step 4). Note that the test stimulus must be minimal because previous exposure to bombykol habituates silkmoths and decreases their sensitivity (Matsuyama and Kanzaki, unpublished data).

4. Odor Source Preparation

Note: Male *B. mori* are sensitive to the major component of the conspecific female sex pheromone (bombykol: (E,Z)-10,12-hexadecadien-1-ol)[20]. Any contamination of experimental equipment with bombykol elicits the odor-tracking behavior and affects the responsiveness of the moth.

1. Drop 10 µl of the bombykol solution dissolved in n-hexane (200 ng/µl) on a piece of filter paper (approximately 10 mm × 10 mm). The amount of bombykol per piece of filter paper is 2,000 ng.
   Note: To check the normal walking behavior of the moth, prepare a pheromone stimulus cartridge in this step. The cartridge is a glass Pasteur pipette with one piece of filter paper containing 2,000 ng of bombykol. Pushing a bulb puffs the air containing bombykol.

5. Odor Source Localization Experiment

1. Turn on the fan of a pulling-air-type wind tunnel (1,800 × 900 × 300 mm, L × W × H; **Figure 8**) and set the wind speed to 0.7 m/sec. Ensure that the temperature is more than 20 °C.
2. Set the odor source (the piece of filter paper containing bombykol) upstream of the wind tunnel.
   Note: The plume width should be confirmed prior to the experiment by using $TiCl_4$ [17,19].
3. Turn on the microcontroller board of the robot and establish a serial connection to a PC via Bluetooth.
4. Launch a custom-made Java program called "BioSignal," which provides an interface between the PC and the robot.
   Note: The main window includes buttons for sending commands to the robot, text windows for displaying the input and output of the serial communication, and small boxes to configure parameters. The subsequent commands are sent by clicking corresponding buttons in this program, except for video capturing.
5. Click on the "about device" button to confirm the connection by sending a command to the robot via the specified COM port and check that a message is returned by the robot.
6. Click on the "memory erase" button to erase previous locomotion data left on the onboard flash memory.
7. Click on the "drivemode1" button to send the default motor gains to the robot.
   Note: The manipulations of the motor gains and the time delay between insect locomotion and robot movement are applied after this step (see steps 6.1 and 6.3, **Figure 9**).
8. Click on the "don't drive" button to send a command to immobilize the robot until the experiment starts.
9. Put the robot at a start position (600 mm downstream from the odor source) and turn on the switch of the motor driver board.
10. Push the recording button of the camcorder to start video capture.
11. Click on the "rec start" button to send a start command to initiate the robot with a simultaneous recording of the ball rotation on the onboard flash memory. Observe that the robot starts to move and tracks the odor plume.
12. Click on the "rec stop" and "don't drive" buttons to send commands to stop both the robot movement and the recording if the robot localizes the odor source.
13. Push the recording button of the camcorder to stop video capture.
14. Download recorded locomotion data from the onboard flash memory to the computer via a serial connection. Close the program.

6. Manipulation of the Insect-controlled Robot

Note: The timing of each manipulation is indicated in **Figure 9**.

1. Manipulation of motor gains
   Note: This manipulation alters the translational and rotational velocity of the robot. Asymmetrical motor gains generate a turning bias, which can be used to investigate how insects compensate for the bias[17].
   1. Define the rotational gains for forward and backward rotation of the motor on each side[17] (**Figure 6B**) by editing the configuration file named "param2.txt" using a text editor.
   2. Click on the "set param2" to read the edited configuration file in the software program. Then, click on the "drivemode2" to send the manipulated gains to the robot.

2. Inversion of the motor output
   Note: This manipulation provides a condition similar to the inversion of bilateral olfactory input (see step 6.4) and can be used to investigate the significance of bilateral olfaction. However, the inversion of motor output also inverts self-induced visual motion of an onboard moth. The impact of the inverted self-induced visual input can be evaluated by a comparison with the inverted olfactory input[19].
   1. Invert the bilateral motor control by crossing the control cables for each motor.

3. Manipulation of the time delay between insect locomotion and robot movement.
   Note: This manipulation allows for the investigation of the acceptable period of time spent on sensory-motor processing for the robotic odor-tracking. The microcontroller stores the locomotion data on a buffer memory and then processes it after the specified time delay. Note that the robot has a maximal internal time delay of 200 msec; therefore, the actual time delay is expected to be the specified time delay plus 200 msec[16,17].
   1. Input a number (from 0-10) in a small box of the main window to specify a time delay from 0-1,000 msec at 100-msec steps.
   2. Click on the "set delay" button to apply the time delay.

4. Manipulation of the olfactory input.
   Note: This manipulation can be used to investigate the significance of bilateral olfactory input. The surge direction of silkmoths is biased on the higher-concentration side[22].

1. Change the gap between the suction tube tips or invert their positions to alter the difference in odor concentration acquired by each antenna.

5. Manipulation of visual input
Note: This manipulation is to investigate the role of visual input for odor-tracking.
1. Cover the canopy with a white paper that occludes 105° and 90° of the horizontal and vertical visual field of the onboard moth, respectively.

Representative Results

We present here the basic characteristics of the insect-controlled robot required for the successful localization of an odor source. The comparison between the robot and silkmoths, the effectiveness of the odor delivery system, and the significance of accurate bilateral olfactory and visual inputs are examined.

The comparison of odor-tracking behaviors between freely-walking moths and the insect-controlled robot is shown in **Figure 10A** and **B**. Under the same odor circumstances, both the walking moths and the robots scored success rates of 100% (walking moth, 10 trials by *N* = 10 moths; robot, 7 trials by *N* = 7 moths). Though the robot exhibited broader trajectories compared to those of the walking moths, there was no significant difference in the time to localization between the walking moths and the robot ($P > 0.05$, Wilcoxon rank sum test; moth, median = 46.5 sec, IQR = 36.7, 69.6; robot, median = 48.1 sec, IQR = 44.9, 61.9).

The odor delivery system (**Figure 5B**) is necessary for supplying the odorant flow near the floor to the antennae of the onboard moth placed 90 mm above the floor. Without this system (suction tubes, fans, and the canopy), the robot could not orient toward the odor source and continued circling until it stopped (all 10 trials by *N* = 5 moths failed, **Figure 10C**). According to programmed silkmoth behavior, continuous circling is a typical behavior when a silkmoth fails to contact the pheromone during orientation[21,22].

Figure 11 shows the representative results demonstrating the manipulations of the robot. The effectiveness of a bilateral olfactory input for odor-tracking was evaluated by changing the position of the tube tips (step 6.4) or by inverting the motor output (step 6.2). The robot achieved success rates of 100% with two different gaps between the left and right tubes (wide gap [control], 90 mm, 10 trials by *N* = 10 moths; narrow gap, 20 mm, 10 trials by *N* = 10 moths; **Figure 11A**, **B**), and there was no significant difference in the time to localization between these two tube positions ($P > 0.05$, Steel's test; **Figure 11E**). On the other hand, the inversion of tube tips (each antenna received the odorant from the contralateral side, tube gap = 90 mm) broadened trajectories along the crosswind direction and slightly increased the median of time to localization, although there was no significant difference ($P > 0.05$, Steel's test; **Figure 11C**, **E**). The inversion of motor output provides a similar situation as the inverted olfactory input; furthermore, it also inverts the self-induced visual motion received by the onboard moth. Because of the inverted negative visual feedback (*i.e.,* positive feedback), the robot continued circling, even in the odor plume (**Figure 11D**), which significantly lengthened the time to localization ($P < 0.01$, Steel's test; **Figure 11E**). The success rates of the inverted olfactory input (C) and the inverted motor output (D) were 80% (10 trials by N = 10 moths) and 90.9% (11 trials by 11 moths), respectively. A detailed discussion of sensory-motor control in silkmoths is described in the previous work[19].

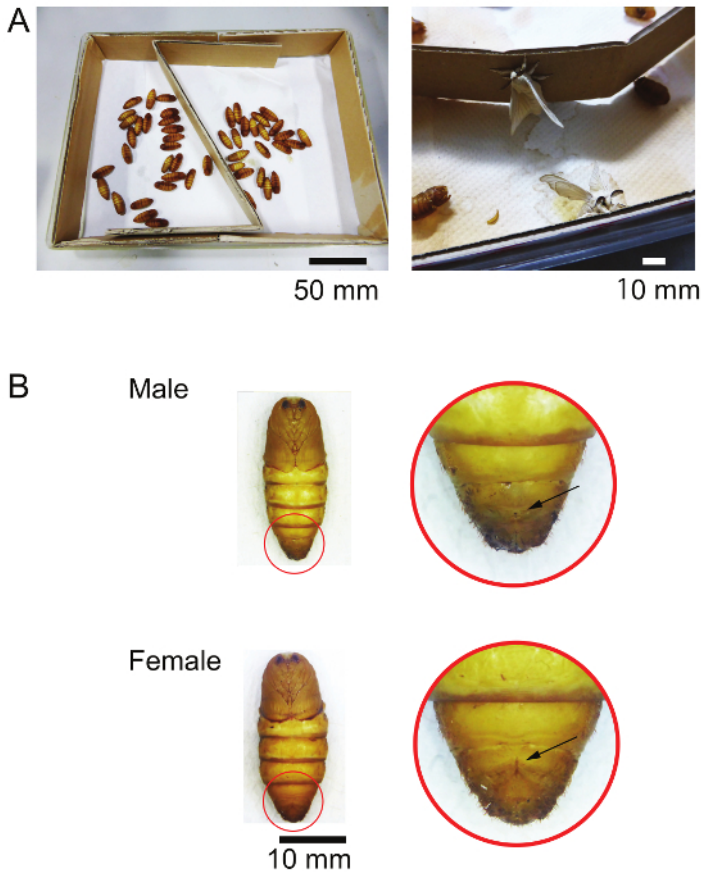

Figure 1. Storing of silkmoth pupae. (**A**) Male pupae are stored in a plastic box (left). The adult moths hold the cardboard around the inner wall of the box during eclosion (right). (**B**) Sex markings of pupae. Each arrow indicates a small spot on the ventral side of ninth abdominal segment of the male and an "X" mark with a fine, longitudinal line on the ventral side of the eighth abdominal segment of the female. Please click here to view a larger version of this figure.

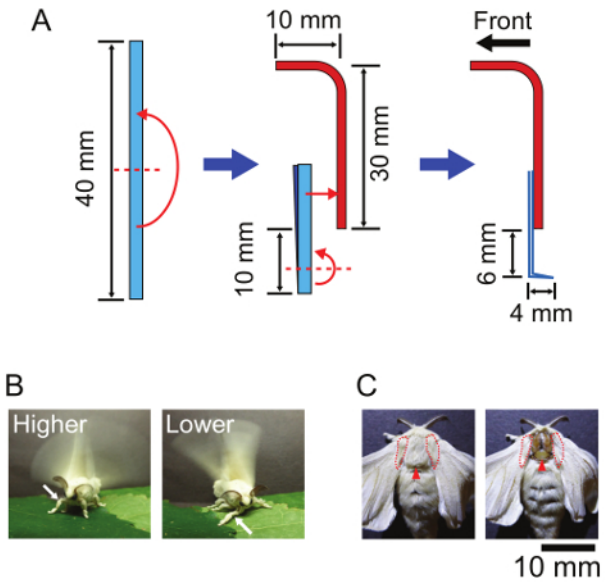

Figure 2. Tethering a silkmoth. (**A**) Fabrication of an attachment for tethering a silkmoth. The three steps are described in 2.1.1 to 2.1.3 (see text). A two-fold strip of thin plastic sheet was attached at the tip of the copper wire, which absorbs the dorsal-ventral movement (see **Figure 2B**) of the mesonotum during walking. The other, curved tip of the wire is for handling. (**B**) Higher and lower attitudes of a silkmoth during pheromone tracking (see the angle between the femur and the tibia of the forelegs [arrows]). (**C**) Removal of the scales on the mesonotum (indicated by arrowheads). The left and right pictures show before and after the removal of scales, respectively. The forewing tegulae were intact (surrounded by dashed lines). Please click here to view a larger version of this figure.

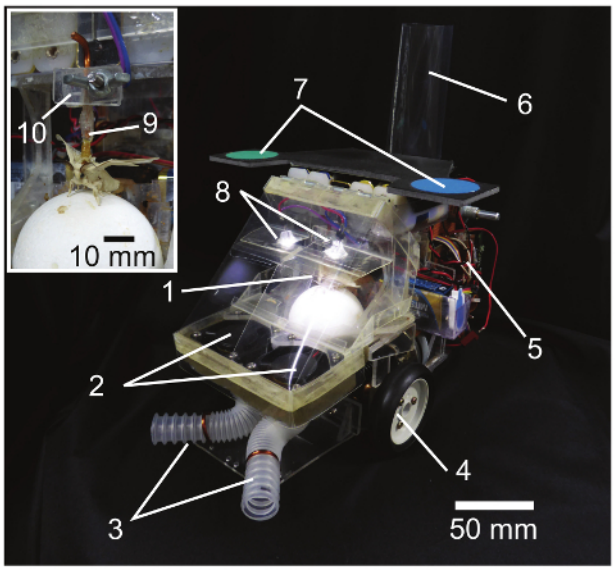

Figure 3. Insect-controlled robot. The inset shows a magnified view of the cockpit. (1) A tethered silkmoth on a treadmill (an air-supported ball, see inset), (2) two fans for supplying an odor to the moth (air speed, 0.5 m/sec), (3) suction tubes for taking the odor, (4) DC motors and wheels, (5) microcontroller boards, (6) an air intake for supplying air to the ball, (7) tracking markers for offline video analyses, (8) two LEDs to keep constant illumination in the cockpit (280 lx), (9) an attachment for tethering the silkmoth, and (10) a fixture of the attachment. Please click here to view a larger version of this figure.

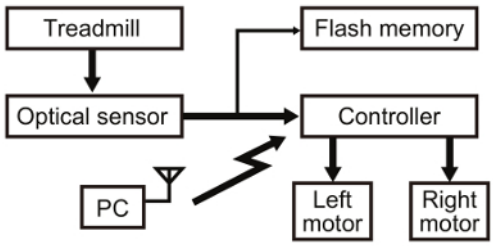

Figure 4. Hardware diagram. The rotation of the air-supported ball in the treadmill was measured by an optical mouse sensor with a resolution of 0.254 mm at a sampling rate of 1.5 kHz. The microcontrollers calculated the trajectory of the silkmoth from the sensor output and controlled two DC motors on the left and right sides. The motors were driven by pulse-width modulation at 1 kHz, with position feedback from built-in Hall sensors. The optical sensor output (*i.e.,* behavior of the onboard moth) was stored on an onboard flash memory (8 Mbit) at a sampling rate of 5 Hz. These data were used for comparing the behavior of the onboard moth with robot movements. The wireless communication between a computer (PC) and the robot was achieved via Bluetooth, which was only used for sending commands to start and stop the robot, or to manipulate the motor properties of the robot. Please click here to view a larger version of this figure.

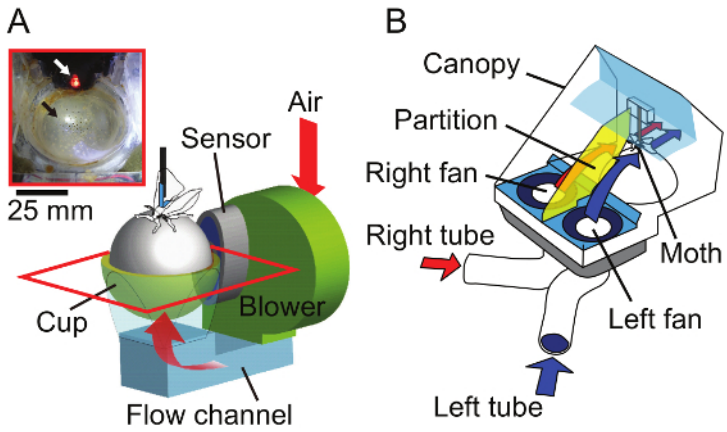

Figure 5. Airflow designs for the treadmill and the odor delivery system. (**A**) Airflow to support the ball of the treadmill. The air was taken from the air intake behind the cockpit by a blower fan; it then flowed through a channel and blew out from small holes (1-mm diameter) on a custom-made FRP cup (inset). The top view of the cup surrounded by a red rectangle is shown in the inset. Red arrows indicate airflow; the white arrow, the optical sensor with an LED transmitter; and the black arrow, the cup with small holes. (**B**) The airflow of the odor delivery system. The air containing the pheromone was suctioned from the tip of a flexible polyethylene tube on each side, separated with a partition in the canopy, and delivered to the antenna on the ipsilateral side. Airflow on each side is indicated by red or blue arrows. This figure has been modified from Ando and Kanzaki[19]. Please click here to view a larger version of this figure.

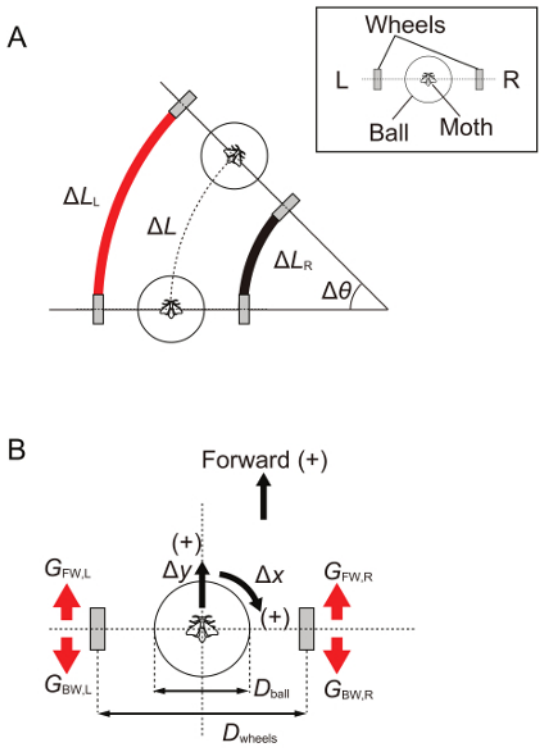

Figure 6. Calculation of the robot movement from insect locomotion. (**A**) A schematic drawing of the robot (ΔL) and wheel movements (left, ΔL_L and right, ΔL_R). $\Delta\theta$, turn angle of the robot. (**B**) Parameters for the calculation. Δx and Δy represent the rotational and translational movements of a ball (a positive value indicates the clockwise or forward direction); D_{ball}, the diameter of the ball; D_{wheels}, the distance between wheels; $G_{FW,L}$ and $G_{BW,L}$, motor gains of forward (FW) or backward (BW) rotation of the left wheel (L); $G_{FW,R}$ and $G_{BW,R}$, motor gains of forward or backward rotation of the right wheel (R). Please click here to view a larger version of this figure.

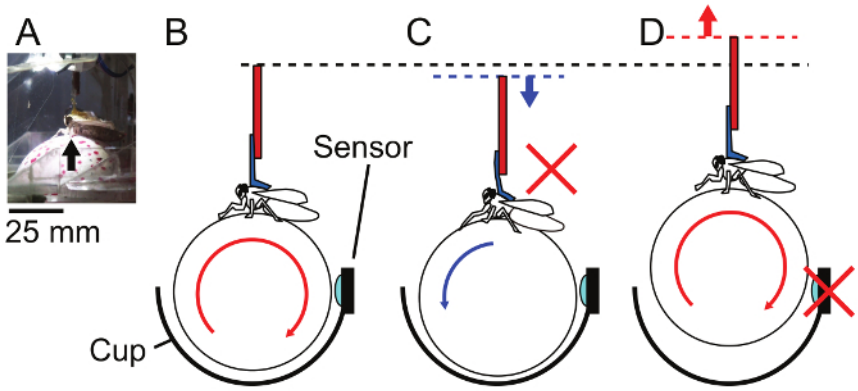

Figure 7. Adjustment of the position of a tethered moth on the treadmill. (**A**) The lateral view of a tethered moth on a ball. The middle legs should be placed at the top of the ball (black arrow). (**B**) The appropriate vertical position of the moth. The optical sensor behind the moth faces the center of the ball. Normal forward walking rotates the ball clockwise (as viewed from the left side). (**C**) The vertical position is too low (downward arrow). The silkmoth extends the forelegs to resist the pressures and rotates the ball backward (counterclockwise rotation). (**D**) The vertical position is too high (upward arrow). The moth holds the ball and lifts it up. Although the moth can perform forward walking in this situation[23] (clockwise rotation), it lifts up the ball and shifts its position. The vertical shift of ball position increases the gap between the ball and the optical sensor, which results in a failure of sensor reading. Please click here to view a larger version of this figure.

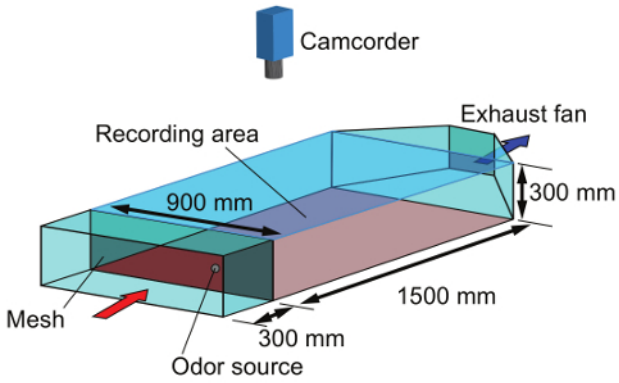

Figure 8. Wind tunnel. The air was filtered with a mesh panel (red arrow); it then entered the recording area of a camcorder, 1,500 (L) × 900 (W) mm. The odor source was placed upstream of the recording area and the pheromone-contaminated air was exhausted outside by a fan (blue arrow). The wind tunnel was made of extruded polystyrene foam. The ceiling was a transparent acrylic sheet, and the floor was a rubber mat to avoid slipping of the robot wheels. The odor source was placed at the center of the crosswind position and 250 mm downwind from the mesh panel. Please click here to view a larger version of this figure.

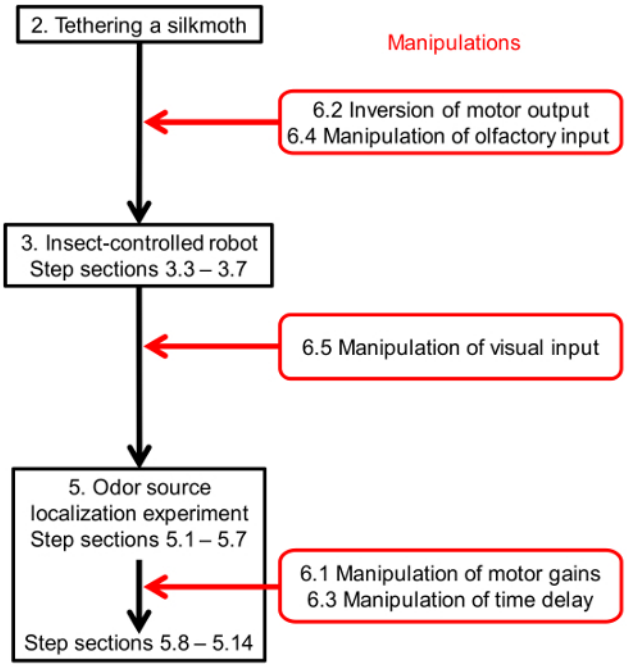

Figure 9. Timings of manipulations of the robot in the protocol. Please click here to view a larger version of this figure.

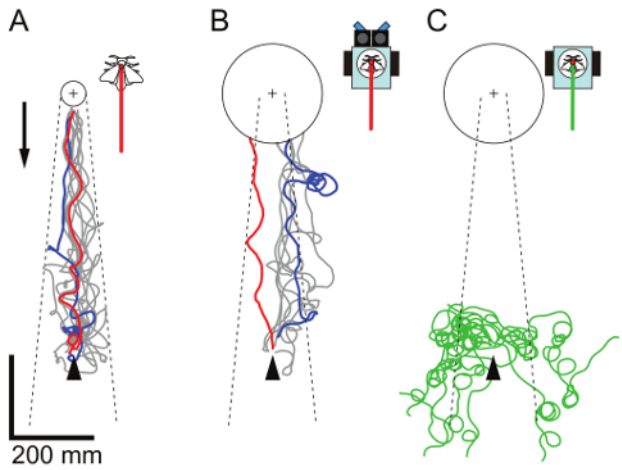

Figure 10. Odor source localization test. Each panel shows the trajectories of the silkmoths (**A**; 10 trials by *N* = 10 moths; data from Ando *et al.*[17]), the insect controlled robot (**B**; 7 trials by *N* = 7 moths), and the robot without the odor delivery system (**C**; 10 trials by *N* = 5 moths). The moths or the robot started 600 mm downwind (arrowhead) from an odor source (cross mark, a piece of filter paper containing 2,000 ng of bombykol). The trials with the shortest or the longest time taken for localization are indicated as red and blue lines, respectively. The other successful trials are colored gray, and failed trials are green. A circle indicates the goal area for judging success in localization. The radius of the goal area was defined on the basis of the size of the robot, equivalent to the closest distance between the onboard moth and the odor source[17]. An arrow indicates wind direction (wind speed: 0.7 m/sec), and dashed lines indicate the boundaries of the pheromone plume. Please click here to view a larger version of this figure.

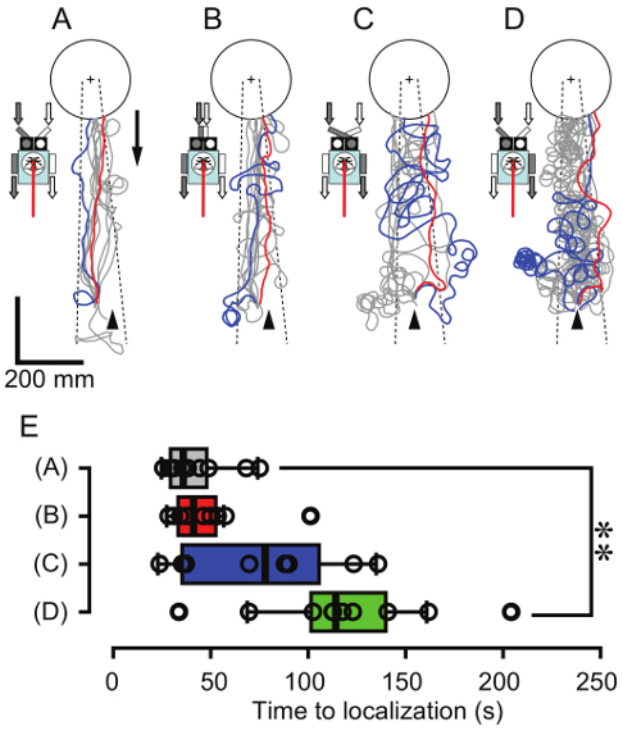

Figure 11. Manipulation of the olfactory input and the motor output. Each panel shows successful trajectories of the robot (the position of the onboard moth) with a wide-tube gap (**A**; control, 90 mm, successful in all 10 trials by *N* = 10 moths), a narrow gap (**B**; 20 mm, successful in all 10 trials by *N* = 10 moths), an inverted wide-tube gap (**C**; successful in 8 of 10 trials, *N* = 10 moths), and a wide-tube gap with inverted motor output (**D**; successful in 10 of 11 trials, *N* = 11 moths). The repetitive air puffs through a piece of filter paper containing 2,000 ng of bombykol were released from the cross mark. The gray and white arrows with the robot indicate the orientations of bilateral olfactory input and motor output. The other experimental conditions and figure descriptions are the same as in **Figure 10**. (**E**) Time to localization of the robot under the four conditions (A-D). Individual data are summarized in a box plot. The left and right sides of the box indicate the first and third quartiles, and the bar represents the median. The whiskers indicate the 1.5× interquartile range. Asterisks indicate a significant difference from the control data (A), according to Steel's test (**P < 0.01). Please click here to view a larger version of this figure.

Discussion

The most important points for the successful control of the robot by a silkmoth are letting the moth walk smoothly on the air-supported ball and the stably measuring the ball rotation. Therefore, tethering the silkmoth and mounting it on the ball at the appropriate position are the critical steps in this protocol. Inappropriate adhesion of the moth to the attachment or inappropriate positioning of the moth on the ball will cause unnatural pressure on it, which perturbs its normal walking behavior and/or causes a failure of the optical sensor to measure the ball rotation. Roughening the polystyrene ball is also important to prevent the moth from slipping. The locomotion of the tethered moth in response to odor stimuli and the subsequent robot movement should be carefully checked prior to the odor-tracking test (see step 3.6).

The use of a larger ball is better because it decreases the curvature of the treadmill, which provides a nearly flat plane for the insect legs. The 50-mm diameter ball used here is relatively small compared to that used in the conventional treadmill setup for silkmoths (diameter: 75 mm)[24]. However, a larger (and heavier) ball must be used with care, because the inertia of the ball is not negligible during robot movements. If an onboard moth cannot restrain the inertial-force-induced rotation of a ball during robot movements by its legs, the robot oscillates continuously without any walking by the moth. When experimenters consider the use of other insect species, therefore, the ball size should be selected on the basis of the strength of their leg grips as well as their sizes. During odor source localization, experimenters should also check the behavior of the moth-whether an onboard moth walks smoothly on the ball and the robot quickly responds as the moth moves. The silkmoth exhibits backward walking when it receives too much pressure from the attachment (a too-low position, see **Figure 7**) and repetitive movements of the forelegs if they slip on the ball or touch an object (such as the partition in front of the head, **Figure 5B**). Poor responsiveness of the robot to insect locomotion is due to inappropriate ball position or the depletion of the batteries (the batteries last for approximately 30 min).

The limitation of the insect-controlled robot is that the onboard moth is definitely situated under unnatural circumstances. The treadmill, the odor delivery system, and the 90-mm height of the cockpit provide different sensory information (mechanosensory, olfactory, and visual) from those acquired by freely-walking moths. These differences became obvious when we compared the behaviors of the insect-controlled robot with those of freely-walking silkmoths. For example, though the same performance for odor source localization was observed between the robot and freely-walking silkmoths, the trajectories of the robot were sparse along the crosswind direction, whereas those of the freely-walking silkmoths converged as they reached the odor source, according to the decrease of plume width (**Figure 10A**, **B**). This difference is simply due to the different sizes of the robot and moths. In particular, the distance between the onboard moth and the tube tip determines the range for searching odorants; therefore, the larger distance (robot: 100 mm; moth: approximately 10 mm from the thorax to the antenna tip) enable the robot to activate even outside the plume. Furthermore, the moth in the canopy cannot receive the wind direction from the external environment. Although the significance of the wind direction for odor-tracking has not yet been determined in silkmoths[22], the use of flow direction is a fundamental strategy for odor-tracking in other organisms[5,6]. Because of the imposed airflow generated by the odor delivery system, it is also difficult to account for "active sensing," such as the effect of wing flapping that generates airflow and facilitates odor reception in silkmoths[25]. Because of these limitations, if experimenters employ this technique to explore the use of multiple modalities, it should be discussed whether the results obtained by these robot experiments can be applied to intact insects in natural conditions[19].

The insect-controlled robot fulfilled three requirements for the evaluation of the odor-tracking capability of insects: 1) direct interfacing of insect motor commands to robot control, 2) testing in a real odor plume, and 3) allowing the manipulation of the insect's sensory-motor system. First, regarding the interface between an insect and a robot, the use of neural signals for controlling a robot, such as a brain-machine interface[26], is an alternative technique. Several studies on insects use neural signals or electromyograms for control of a robot and closed feedback loops[27-30]. However, this approach requires the decoding of neural signals to extract meaningful motor commands, which is an important and ongoing research subject in neuroscience. Therefore, the use of actual walking behavior of insects for robot control is a direct and simple way to interface the insect's motor commands to a robot. Second, regarding the environment in which the robot behaves, the use of virtual reality would be an alternative[13,31-33]. Virtual reality enables us to conduct behavioral experiments under more controlled situations and is most successful in the study of vision, where the air-supported treadmill has been used for tracking animal locomotion and generation of visual circumstances[24,34-36]. However, closing the feedback loop of olfactory information is technically difficult because it requires precise flow control. Although the application of optogenetics to activate olfactory receptor neurons[37-40] will overcome the limitations of virtual reality in olfaction, the use of a mobile robot in a real odor plume would be a reliable way to establish an olfactory closed loop at present. Finally, regarding the manipulation of an insect's sensory-motor system, alternative approaches would be surgical manipulations of the insects (*i.e.,* cutting or covering sensory organs or appendages[41]). However, our robotic manipulation (step 6 and **Figure 11**) is a non-invasive and reversible way to alter the sensory-motor system of insects, achieved by the manipulation of the robot platform[19], and the controllability of various parameters of the robot enables us to test its performance under various circumstances.

The insect-controlled robot has two major directions for future applications. The first direction is for engineering. As an autonomous robot controlled by the insect sensory-motor system, the insect-controlled robot will be a reference for mobile robots implemented with biological models, ranging from simplified Braitenberg vehicles[42] to large-scale neural networks. The insect-controlled robot will also be a useful platform for testing possible combinations of other modalities with insect odor-tracking, such as the implementation of a camera and an algorithm for collision avoidance to explore collision-free odor-tracking algorithms. Furthermore, fine-tuning of the robot properties may improve the odor-tracking performance better than intact insects. Such translation of the insect capability might lead to the practical use of this robot itself for finding hazardous materials, if we imitate the transgenic silkmoths[43] that respond to characteristic chemicals in a target material. On the other hand, the insect-controlled robot will also raise an important question: How should we use biomimetic algorithms for robotic applications that extend beyond the difference between insects and robots? For example, insect olfactory receptors have an outstanding ability to acquire high-speed temporal dynamics of odor concentration[44-46], which is responsible for insect olfactory processing and odor source localization, but are far beyond the capabilities of conventional gas sensors[4,29,47]. How to modify the biomimetic algorithm to meet the sensory ability of robots should also be explored as a future direction. The other major direction is definitely for biology. The insect-controlled robot can be regarded as a closed-loop experimental platform. In addition, robotic manipulation, a non-invasive way to alter the insect's sensory-motor relationship, will be further applied to investigate how the small insect brain can respond, learn, and adapt to new circumstances.

Disclosures

The authors have nothing to disclose.

Acknowledgements

We thank Shigeru Matsuyama for providing purified bombykol. This work was supported by the Japan Society for the Promotion of Science KAKENHI (grant numbers 22700197 and 24650090) and the Human Frontier Science Program (HFSP).

References

1. Murlis, J., & Jones, C. D. Fine-scale structure of odor plumes in relation to insect orientation to distant pheromone and other attractant sources. *Physiol Entomol.* **6**, 71-86 (1981).
2. Vergassola, M., Villermaux, E., & Shraiman, B. I. 'Infotaxis' as a strategy for searching without gradients. *Nature.* **445**, 406-409 (2007).
3. Kowadlo, G., & Russell, R. A. Robot Odor Localization: A Taxonomy and Survey. *The International Journal of Robotics Research.* **27**, 869-894 (2008).
4. Hernandez Bennetts, V., Lilienthal, A. J., Neumann, P. P., & Trincavelli, M. Mobile robots for localizing gas emission sources on landfill sites: is bio-inspiration the way to go? *Frontiers in neuroengineering.* **4**, 20 (2011).
5. Vickers, N. J. Mechanisms of animal navigation in odor plumes. *Biol Bull.* **198**, 203-212 (2000).
6. Willis, M. A. Chemical plume tracking behavior in animals and mobile robots. *Navigation.* **55**, 127-135 (2008).
7. Carde, R. T., & Willis, M. A. Navigational strategies used by insects to find distant, wind-borne sources of odor. *J Chem Ecol.* **34**, 854-866 (2008).
8. Frye, M. A. Multisensory systems integration for high-performance motor control in flies. *Curr Opin Neurobiol.* **20**, 347-352 (2010).
9. Russell, R. A. Survey of robotic applications for odor-sensing technology. *The International Journal of Robotics Research.* **20**, 144-162 (2001).
10. Russell, R. A., Bab-Hadiashar, A., Shepherd, R. L., & Wallace, G. G. A comparison of reactive robot chemotaxis algorithms. *Robot Auton Syst.* **45**, 83-97 (2003).
11. Ishida, H., Nakamoto, T., Moriizumi, T., Kikas, T., & Janata, J. Plume-tracking robots: a new application of chemical sensors. *Biol Bull.* **200**, 222-226 (2001).
12. Webb, B., Harrison, R. R., & Willis, M. A. Sensorimotor control of navigation in arthropod and artificial systems. *Arthropod Struct Dev.* **33**, 301-329 (2004).
13. Kanzaki, R. How does a microbrain generate adaptive behavior? *Int Congr Ser.* **1301**, 7-14 (2007).
14. Kanzaki, R., Ando, N., Sakurai, T., & Kazawa, T. Understanding and reconstruction of the mobiligence of insects employing multiscale biological approaches and robotics. *Adv Robotics.* **22**, 1605-1628 (2008).
15. Ravel, N. *et al.* Multiphasic on/off pheromone signalling in moths as neural correlates of a search strategy. *Plos One.* **8**, e61220 (2013).
16. Emoto, S., Ando, N., Takahashi, H., & Kanzaki, R. Insect-controlled robot-evaluation of adaptation ability. *J Robot Mechatronics.* **19**, 436-443 (2007).
17. Ando, N., Emoto, S., & Kanzaki, R. Odour-tracking capability of a silkmoth driving a mobile robot with turning bias and time delay. *Bioinspir Biomim.* **8**, 016008 (2013).
18. Gatellier, L., Nagao, T., & Kanzaki, R. Serotonin modifies the sensitivity of the male silkmoth to pheromone. *J Exp Biol.* **207**, 2487-2496 (2004).
19. Ando, N., & Kanzaki, R. A simple behaviour provides accuracy and flexibility in odour plume tracking - the robotic control of sensory-motor coupling in silkmoths. *J. Exp. Biol.* **218**, 3845-3854 (2015).
20. Kaissling, K. E. Insect olfaction. in *Handbook of Sensory Physiology.* Vol. 4 (ed L. M. Beidler) 351-431 Springer-Verlag, (1971).
21. Kanzaki, R., Sugi, N., & Shibuya, T. Self-generated zigzag turning of *Bombyx mori* males during pheromone-mediated upwind walking. *Zool Sci.* **9**, 515-527 (1992).
22. Takasaki, T., Namiki, S., & Kanzaki, R. Use of bilateral information to determine the walking direction during orientation to a pheromone source in the silkmoth *Bombyx mori. J Comp Physiol. A* **198**, 295-307 (2012).
23. Kanzaki, R. Coordination of wing motion and walking suggests common control of zigzag motor program in a male silkworm moth. *J Comp Physiol A.* **182**, 267-276 (1998).
24. Pansopha, P., Ando, N., & Kanzaki, R. Dynamic use of optic flow during pheromone tracking by the male silkmoth, *Bombyx mori. J Exp Biol.* **217**, 1811-1820 (2014).
25. Loudon, C., & Koehl, M. A. R. Sniffing by a silkworm moth: Wing fanning enhances air penetration through and pheromone interception by antennae. *J. Exp. Biol.* **203**, 2977-2990 (2000).
26. Lebedev, M. A., & Nicolelis, M. A. L. Brain-machine interfaces: past, present and future. *Trends Neurosci.* **29**, 536-546 (2006).
27. Ejaz, N., Peterson, K. D., & Krapp, H. G. An experimental platform to study the closed-loop performance of brain-machine interfaces. *Journal of visualized experiments : JoVE.* (2011).
28. Minegishi, R., Takashima, A., Kurabayashi, D., & Kanzaki, R. Construction of a brain-machine hybrid system to evaluate adaptability of an insect. *Robot Auton Syst.* **60**, 692-699 (2012).
29. Martinez, D., Arhidi, L., Demondion, E., Masson, J. B., & Lucas, P. Using insect electroantennogram sensors on autonomous robots for olfactory searches. *Journal of visualized experiments : JoVE.* e51704 (2014).
30. Ortiz, L. I. *A mobile electrophysiology board for autonomous biorobotics.* MS thesis, The University of Arizona, (2006).
31. Bohil, C. J., Alicea, B., & Biocca, F. A. Virtual reality in neuroscience research and therapy. *Nat Rev Neurosci.* **12**, 752-762 (2011).
32. Dombeck, D. A., & Reiser, M. B. Real neuroscience in virtual worlds. *Curr Opin Neurobiol.* **22**, 3-10 (2012).
33. Roth, E., Sponberg, S., & Cowan, N. J. A comparative approach to closed-loop computation. *Curr Opin Neurobiol.* **25**, 54-62 (2014).

34. Leinweber, M. *et al.* Two-photon calcium imaging in mice navigating a virtual reality environment. *Journal of visualized experiments : JoVE*. e50885 (2014).
35. Takalo, J. *et al.* A fast and flexible panoramic virtual reality system for behavioural and electrophysiological experiments. *Sci Rep.* **2**, 324 (2012).
36. Bahl, A., Ammer, G., Schilling, T., & Borst, A. Object tracking in motion-blind flies. *Nat Neurosci.* **16**, 730-738 (2013).
37. Bellmann, D. *et al.* Optogenetically Induced olfactory stimulation in *Drosophila* larvae reveals the neuronal basis of odor-aversion behavior. *Front Behav Neurosci.* **4**, 27 (2010).
38. Gaudry, Q., Hong, E. J., Kain, J., de Bivort, B. L., & Wilson, R. I. Asymmetric neurotransmitter release enables rapid odour lateralization in *Drosophila. Nature*. **493**, 424-428 (2013).
39. Tabuchi, M. *et al.* Pheromone responsiveness threshold depends on temporal integration by antennal lobe projection neurons. *Proc Natl Acad Sci U S A.* **110**, 15455-15460 (2013).
40. Schulze, A. *et al.* Dynamical feature extraction at the sensory periphery guides chemotaxis. *Elife.* **4**, e06694 (2015).
41. Duistermars, B. J., Chow, D. M., & Frye, M. A. Flies require bilateral sensory input to track odor gradients in flight. *Curr Biol*. **19**, 1301-1307 (2009).
42. Gomez-Marin, A., Duistermars, B. J., Frye, M. A., & Louis, M. Mechanisms of odor-tracking: multiple sensors for enhanced perception and behavior. *Front Cell Neurosci.* **4**, 6 (2010).
43. Sakurai, T. *et al.* A single sex pheromone receptor determines chemical response specificity of sexual behavior in the silkmoth *Bombyx mori. Plos Genet*. **7** (2011).
44. Tripathy, S. J. *et al.* Odors pulsed at wing beat frequencies are tracked by primary olfactory networks and enhance odor detection. *Front Cell Neurosci*. **4**, 1 (2010).
45. Daly, K. C., Kalwar, F., Hatfield, M., Staudacher, E., & Bradley, S. P. Odor detection in *Manduca sexta* is optimized when odor stimuli are pulsed at a frequency matching the wing beat during flight. *Plos One.* **8**, e81863 (2013).
46. Szyszka, P., Gerkin, R. C., Galizia, C. G., & Smith, B. H. High-speed odor transduction and pulse tracking by insect olfactory receptor neurons. *Proc Natl Acad Sci USA*. **111**, 16925-16930 (2014).
47. Harvey, D., Lu, T. F., & Keller, M. Odor sensor requirements for an insect inspired plume tracking mobile robot. *Proceedings of'The 2006 IEEE International Conference on Robotics and Biomimetics.* 130-135 (2006).

